

## Prediction of salinity intrusion in Danshuei estuarine system

A. Etemad-Shahidi, A. Dorostkar and Wen-Cheng Liu

### ABSTRACT

The main parameters that affect the flow conditions and intrusion of salt water in an estuary system are tides and the seasonal variation of water discharge. A laterally averaged two-dimensional numerical model called MIKE 11 XZ is used to simulate the hydrodynamics and salinity intrusion of Danshuei River estuarine system. This model can simulate hydrodynamics and water quality in estuaries, reservoirs and lakes. MIKE 11 XZ solves the Reynolds-averaged Navier–Stokes equations by using Abbott–Ionescu finite difference scheme in a non-dimensional vertical  $\sigma$ -coordinate. Vertical eddy diffusivity in the model can be determined by a constant value, a mixing length theory and a  $k - \epsilon$  turbulence closure scheme with Richardson number correction. A series of comprehensive field data obtained from Danshuei estuarine system is used for evaluation, calibration and verification of the model. The friction coefficient was calibrated and verified using water surface elevation and velocity measurements, respectively. Then the vertical eddy diffusivity was calibrated and verified through comparison of salinity measurements in different layers of several stations. Reasonable agreement was obtained between the model results and the observed data using  $k - \epsilon$  turbulence closure scheme. The model application was investigated with different discharges and the effect of discharge variation on salinity intrusion was determined. The results showed that the fresh water discharge is the main parameter that affects the salinity intrusion in this system. Finally, simple power equations are suggested to predict the salinity intrusion due to the fresh water discharge in different tributaries of the system.

**Key words** | eddy diffusivity, k-epsilon closure scheme, MIKE 11 XZ, numerical simulation, two-dimensional modelling

**A. Etemad-Shahidi** (corresponding author)  
**A. Dorostkar**  
 School of Civil Engineering and Center for  
 Excellence in Fundamental Studies in Structural  
 Engineering,  
 Iran University of Science and Technology,  
 P.O. Box 16756-163,  
 Narmak, Tehran,  
 Iran  
 E-mail: etemad@iust.ac.ir

**Wen-Cheng Liu**  
 Department of Civil and Disaster Prevention  
 Engineering,  
 National United University,  
 Miao-Li 3600,  
 Taiwan

### NOMENCLATURE

$c$	dissolved or suspended matter concentration	$u$	horizontal velocity
$L$	maximum salinity intrusion length	$w$	vertical velocity
$p$	pressure	$W$	width
$P$	wet perimeter	$\nu_{Tx}$	horizontal eddy diffusivity
$q_0$	lateral inflow	$\nu_{Tz}$	vertical eddy diffusivity
$Q$	flow rate	$\rho_0$	reference density
$Q_{\text{mean}}$	mean flow rate	$\tau_B$	bed shear stress
$Q_{90}$	flow with an exceedance probability of 90%	$\tau_{zx}$	horizontal shear stress
$S_c$	source term	$\Delta t$	time step
$t$	time	$\Delta x$	horizontal grid spacing

doi: 10.2166/nh.2008.107

## INTRODUCTION

Salinity intrusion is one of the most important physical phenomena in estuaries that affect the quality of both surface and ground water. In addition, salinity is the major environmental factor influencing the biodiversity in brackish water (Remane & Schlieper 1971) and its variation determines the diversity of species in estuaries (Attrill 2002). Salt intrusion is influenced by man-made changes on rivers such as dredging, construction of dams and reservoirs and water diversion. The length of salinity intrusion is a suitable indicator of habitats in estuaries since it is well defined and incorporates several important estuarine properties and processes (Jassby *et al.* 1995). The tip of salinity intrusion is also located near spatial maxima in species abundance (Jassby *et al.* 1995) and the estuarine turbidity maxima (Dyer 1997). Different approaches such as field observations, analytical solutions and physical, empirical and numerical models have been used to study and predict the length of salt intrusion. Field observations do not predict the water bodies' behaviour, while analytical solutions are only usable for simple situations. Empirical models are mostly applicable to simplified cases and physical models are too expensive and time-consuming. Numerical models are therefore currently used since they are more usable, flexible and more economic (US Army Corps of Engineers 1991).

In this study, a two-dimensional (2D) laterally averaged model called MIKE 11 XZ is used to simulate the hydrodynamic and salinity intrusion of Danshuei River estuarine system. It has already been shown that this model compares well with analytical solutions (Jakobsen *et al.* 2005). Therefore, we report its first application and verification in a naturally stratified water body. The model was first calibrated and then verified using observed data and the friction and turbulent diffusion coefficients were determined. The verified model was then used to study the effect of hydrological variations on salinity intrusion.

## STUDY AREA

Danshuei estuarine system surrounds Taipei city and is formed by the confluence of the Tahan Stream, Hsintien

Stream and Keelung River. This system is the largest estuarine system in Taiwan (Figure 1) with a total channel length of 327.6 km and a total drainage area of 2,726 km<sup>2</sup> (Hsu *et al.* 1999). The downstream of all three tributaries are influenced by tide and the upriver reaches are affected by daily varying fresh water discharge. The tide spans a total length of about 82 km, surrounding the entire length of the Danshuei River and the downstream reaches of Tahan Stream, the Hsintien Stream and the Keelung River. Normally, the astronomical tide reaches up to Cheng-Ling bridge in Tahan Stream, the Hsiu-Lang bridge in Hsintien Stream and the Chiang-Pei bridge in Keelung River (Figure 1).

The water surface elevation is mainly controlled by tidal propagation. The primary tidal constituent at the river mouth is  $M_2$  tide with a tidal range of 2.17 m and 3 m during mean and spring tides, respectively. The mean tidal range may reach a maximum of 2.39 m within the system due to the cross-sectional contraction and wave reflection (Hsu *et al.* 1999). The wind is not significant in this system because of the presence of high mountains on both sides and the narrowness of the river (Liu *et al.* 2001).

During normal hydrological conditions, vertical stratification exists in at Kuan-Du, Taipei and Pa-Ling bridges (Figure 1). The baroclinic pressure gradient is large enough to push the denser salt water upriver along the bottom layer and the deviation from the classical two-layered circulation only occurs during flood events (Liu *et al.* 2001).

## MEASUREMENTS AND METHODS

### Field measurement

In order to conduct the model calibration and verification, the measured data including water level, longitudinal velocity and salinity were collected from the Water Resources Agency, Taiwan. The automatic record system was installed at the measured stations in the Danshuei River estuarine system to transfer the hourly water level to the Water Resources Agency. Two intensive field measurements were conducted by the Taiwan Water Resources Agency on 12 April and 24 June 1994. Half-hourly current speed and

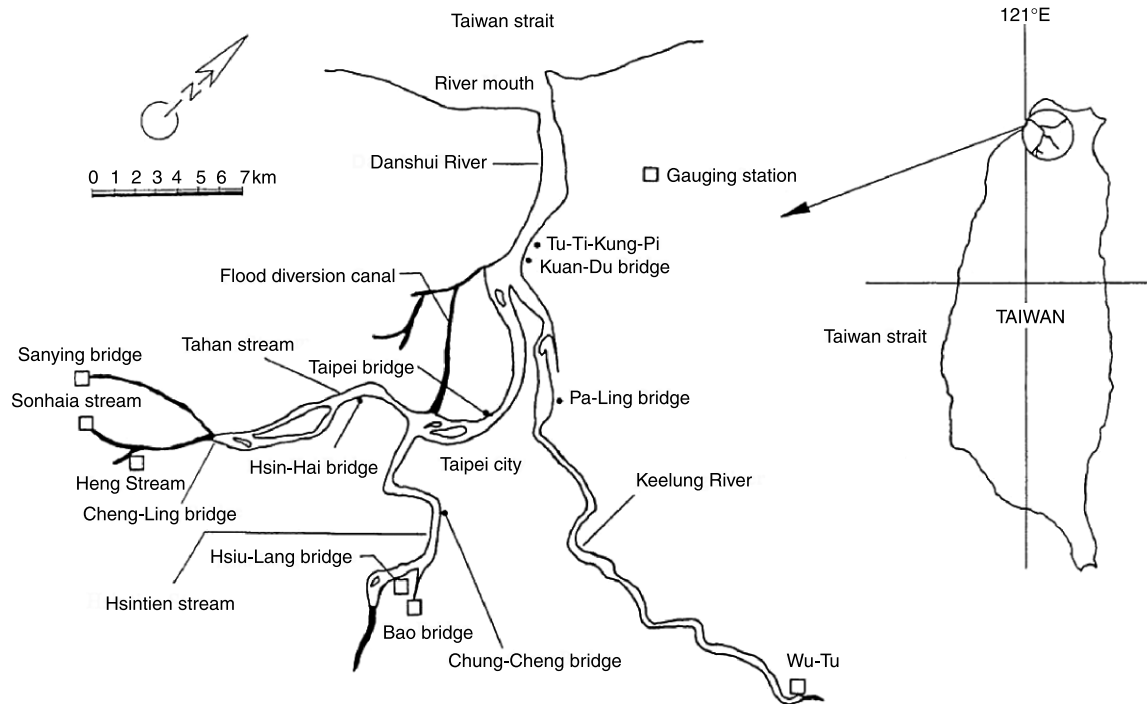


**Figure 1** | Danshuei River estuarine system map and stations.

hourly temperature and salinity were measured by personnel on boats for a period of 13 daylight hours in each case. Velocity data were acquired with handheld current meters that measured the current magnitude but not the direction. The data were recorded by hand and ebb or flood direction was noted visually. There is uncertainty in assessing current direction during the period around slack tides. With the exception of the upriver transects close to tidal limits, the measurements were made at several depths in the vertical direction and several points in the transverse direction. To compare with the results of the vertical 2D model, the data in the transverse direction were averaged to obtain the laterally averaged values. The cross-sectional profiles of the main river and tributaries collected by Taiwan Water Conservation Agency in 1994 through a field survey were used in this study.

### Model description and governing equations

The Abbott–Ionescu finite difference numerical scheme (Abbott & Ionescu 1967) is used in MIKE 11 XZ. The governing equations are laterally integrated continuity,

momentum and transport Equations (Jakobsen *et al.* 2005):

$$\frac{\partial(Wu)}{\partial x} + \frac{\partial(Ww)}{\partial z} = \frac{q_0}{dz} \quad (1)$$

$$W \frac{\partial u}{\partial t} = -\frac{W}{\rho_0} \frac{\partial p}{\partial x} + \frac{\partial(W \frac{\tau_{xx}}{\rho_0})}{\partial z} - \frac{\tau_B}{\rho_0} \frac{\partial P}{\partial z} \quad (2)$$

$$\frac{\partial Wc}{\partial t} + \frac{\partial Wuc}{\partial x} + \frac{\partial Wwc}{\partial z} = \frac{\partial}{\partial x} \left( W \nu_{Tx} \frac{\partial c}{\partial x} \right) + \frac{\partial}{\partial z} \left( W \nu_{Tz} \frac{\partial c}{\partial z} \right) + WS_c \quad (3)$$

respectively, where  $W$  (m) is the width and  $u$  and  $w$  (m/s) are the velocity in the horizontal ( $x$ ) and vertical ( $z$ ) directions, respectively.  $q_0$  ( $\text{m}^3/\text{s}/\text{m}$ ) is the lateral inflow,  $t$  (s) is the time,  $\rho_0$  ( $\text{kg}/\text{m}^3$ ) is the reference density,  $p$  ( $\text{N}/\text{m}^2$ ) is the pressure,  $\tau_{zx}$  ( $\text{N}/\text{m}^2$ ) is the horizontal shear stress,  $\tau_B$  ( $\text{N}/\text{m}^2$ ) is the bed shear stress,  $P$  (m) is the wet perimeter,  $c$  is a dissolved or suspended matter concentration,  $\nu_{Tx}$  and  $\nu_{Tz}$  ( $\text{m}^2/\text{s}$ ) are the horizontal and vertical eddy diffusivities, respectively and  $S_c$  is a source term (Jakobsen *et al.* 2005).

This model is equipped with a constant value, a mixing-length theory and a  $k$  or  $k - \varepsilon$  turbulence closure scheme (e.g. Rodi 1987) to determine vertical eddy diffusivity. All the

equations are transferred and solved in a stretched coordinate system called sigma-coordinate (Slørdal 1997). Complete descriptions of this transformation, the numerical method used for discretizing, bed friction and the governing equations are given by Jakobsen *et al.* (2005).

## MODEL SET-UP, CALIBRATION AND VERIFICATION

The number of vertical layers was 10 for the whole system. The model considers the same thickness for the layers. Hourly tidal water level and daily salinity data from 15 June to 30 September 1994 were used as boundary conditions at the river mouth. The time series of averaged daily river discharge and constant value of 0.001 gr/kg or ppt for salinity were used as upstream boundary condition at the end of tributaries (Hsu *et al.* 1999). A time step of  $\Delta t = 20$  s and a maximum horizontal grid spacing of  $\Delta x = 1,000$  m were used for the numerical simulation and the model was run for the above-mentioned period.

Hsu *et al.* (1999) suggested using the comparison of water levels for calibration of the model and using comparisons of longitudinal velocity for verification of the model. Since friction coefficient is the most important parameter affecting the calculation of the water surface elevation and velocity, time series of water surface elevation were used to calibrate the friction coefficient. The values of Manning's friction coefficients and the absolute mean error

**Table 1** | Manning's friction coefficient and respective absolute mean errors

River	Distance from the mouth (km)	$n$ (s/m <sup>1/3</sup> )	AME (cm)
Tahan-Danshuei	0.0–35.235	0.026	11.34
Tahan-Danshuei	35.235–44.735	0.03	12.39
Tahan-Danshuei	44.735–57.735	0.032	12.4
Hsintien	21.0–36.635	0.015	12.88
Keelung	8.0–38.515	0.023	13.2
Keelung	38.515–52.515	0.016	13.56

(AME) of the modelled water levels in different branches are shown in Table 1. As shown, the absolute mean error (AME) varies from 11.34 to 13.56 cm, i.e. about 5% of the mean tidal range.

It should be noted that the variation of  $n$  is mainly due to the changes in the bed material and artificial alignment made in the system (Hsu *et al.* 1999). The high value of  $n$  is also due to the river bends that cannot be modelled accurately in a 2D simulation. Figure 2 shows the inter-comparison between the modelled and measured water surface elevation at Tu-Ti-Kung-Pi station in August 1994 as a sample. As seen, the model reproduces both phase and amplitude of the tidal variations very well.

To verify the calibrated model, the model results and measured longitudinal velocities were compared at different stations using the calibrated Manning's friction coefficients. Figure 3 shows the results of the comparison at Taipei bridge station on 24 June 1994 as well as results obtained by Hsu *et al.* (1999). As seen, the model reproduces the surface

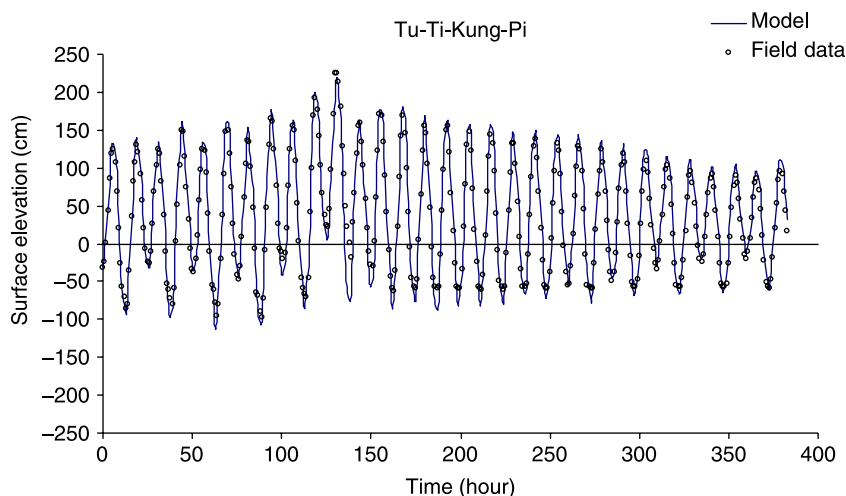


**Figure 2** | Comparison of the computed and measured surface elevations at Tu-Ti-Kung-Pi station, starting from 16 August 1994.

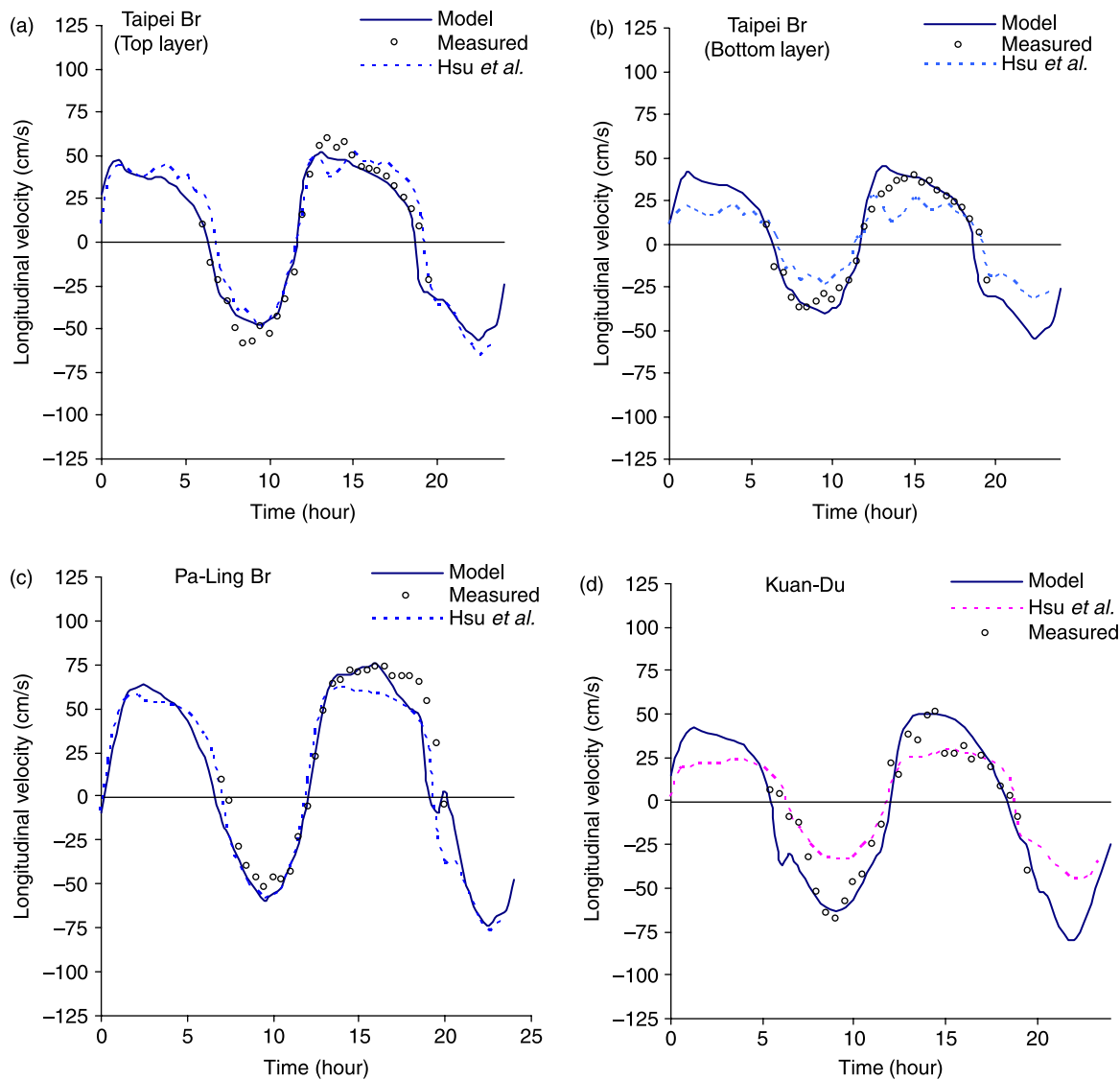


**Figure 3** | Comparison of measured and simulated longitudinal surface velocities on 24 June 1994 at (a) Taipei bridge (surface layer); (b) Taipei bridge (bottom layer); (c) Pa-Ling bridge (surface layer); and (d) Kuan-Du station (bottom layer).

and bottom velocities with AMEs of 7.23 cm/s and 6.2 cm/s, respectively. It outperforms simulations of Hsu *et al.* (1999) using mixing length concept. In this respect, comparisons of velocities at other stations are displayed in Figures 3(c–d) and 4(a–b), highlighting the good performance of the model and the used closure scheme.

The AMEs of velocity comparisons vary between 6.22 cm/s and 13.34 cm/s at different stations (Table 2). As shown, the errors are within the acceptable range considering the uncertainties in both measurements and averaging in a 2D model. It should be noted that the

measurements made at several depths and several points in the transverse direction were used to obtain the laterally averaged values.

Salinity can be used as an ideal natural tracer for calibration of mixing process in most estuaries with a significant freshwater discharge (Hsu *et al.* 1999). The salinity measurements from 15 March to 24 June 1994 were used for calibration of mixing processes. The tidally averaged and time series of measured salinity on 12 April 1994 were used to calibrate the longitudinal eddy diffusivity. The calibrated longitudinal dispersion coefficients are

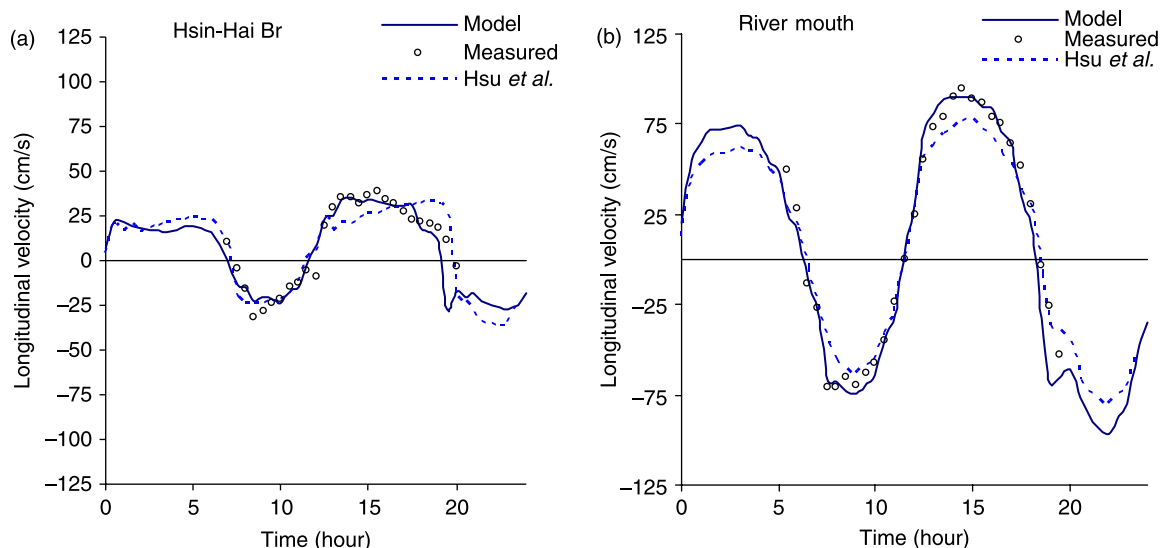


Figure 4 | Comparison of measured and simulated longitudinal bottom velocity on 24 June 1994 at (a) Hsin-Hai bridge; and (b) river mouth (top layer).

120 m<sup>2</sup>/s, 5 m<sup>2</sup>/s and 35 m<sup>2</sup>/s for Tahan Stream, Keelung River, and Hsintien Stream, respectively, which are within the range observed in other estuaries (e.g. Fischer et al. 1979).

It should be noted that the horizontal length scales in estuaries are several orders of magnitude larger than the vertical length scales. Therefore, the horizontal mixing has a minor role in the transport processes (Liu et al. 2007) and constant values of longitudinal eddy diffusivity were used in the simulations. The vertical eddy diffusivity was determined using different turbulence closure schemes and the best results were obtained when the *k* –  $\epsilon$  closure scheme was invoked.

Figure 5 shows the comparison between simulated and measured surface salinities at Pa-Ling station on 12 June 1994. Here, the AME is less than 1 gr/kg or ppt. The inter-comparison of temporal variation of salinities at different stations used for verification is shown in Figures 6 and 7. Again, good qualitative agreements are seen in the figures.

The improved performance of the model, compared to that used by Hsu et al. (1999), is mainly due to the higher order turbulence closure scheme employed in this simulation. The AMEs of the simulation are shown in Table 3, and vary from 0.08 to 0.45. The AME of Hsin-Hai station is lower than the AMEs of other stations but this could be the result of the negligible overall salinity at that station. The simulated and measured salinities on 24 June 1994 are computed for different layers and stations to verify the calibrated vertical eddy diffusivities (Figure 7(a–b)).

### MODEL APPLICATION

The length of the salinity intrusion is a suitable indicator of habitats in estuaries since it is well defined and incorporates several important estuarine properties and processes (Jassby et al. 1995). The verified model was therefore used to investigate the salinity intrusion under five hydrological

Table 2 | Comparison of measured and simulated longitudinal velocities, in the form of AMEs (cm/s), on 24 June 1994

	Hsin Hai		Taipei		Kuan-Du		Pa-Ling		River Mouth	
	MIKE 11 XZ	Hsu et al. (1999)	MIKE 11 XZ	Hsu et al. (1999)	MIKE 11 XZ	Hsu et al. (1999)	MIKE 11 XZ	Hsu et al. (1999)	MIKE 11 XZ	Hsu et al. (1999)
Surface	6.32	8.53	7.23	9.71	13.16	14.34	10.46	14.18	8.96	9.67
Bottom	–	–	6.2	10.51	11.1	11.21	11.6	12.34	5.41	6.66

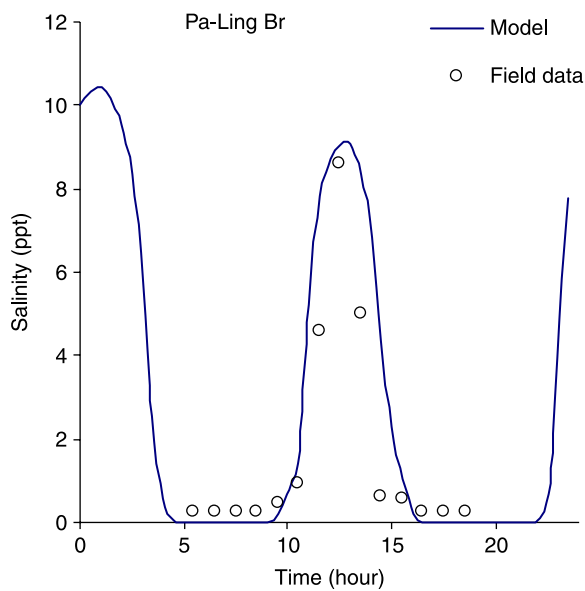


**Figure 5** | Comparison of measured and simulated salinities on 12 April 1994 at Pa-Ling station (1 m below surface water).

conditions varying from mean discharge to  $Q_{90}$ , which is a flow with an exceedance probability of 90% (Table 4). A salinity of 32 ppt at the river mouth was used for all scenarios as the downstream boundary condition. Both the maximum salinity intrusion length and averaged salinity over a 3 day period of spring and neap tides were used to investigate the effects of fresh water discharge variations on salinity intrusion. The limit of salinity intrusion was defined

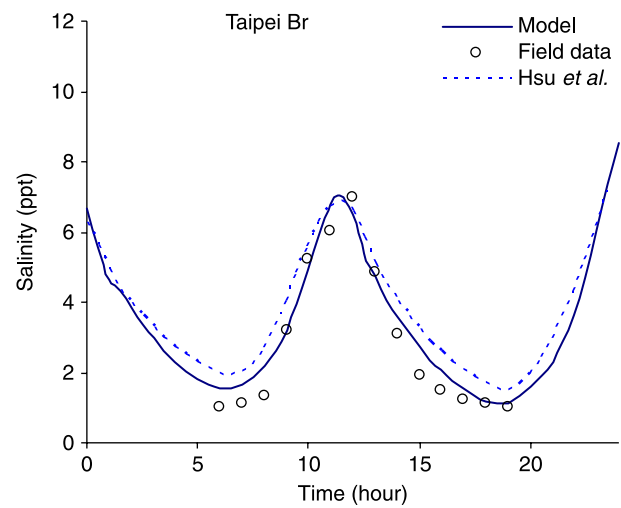


**Figure 6** | Comparison of measured and simulated salinities on 24 June 1994 at Taipei bridge (7.5 m below surface water).

where the salinity is 1 ppt greater than that upstream (Van Der Tuin *et al.* 1991).

The results of simulations show that for  $Q_{\text{mean}}$  conditions, the salt water intrudes about 14 km from the main river mouth and 4 km from the Keelung River mouth at spring tide. Under these conditions, salt water rarely intrudes to Hsintien Stream. During neap conditions, the salinity intrusion limit is about 2 km and 3 km less than that of the spring condition at Tahan Stream and Keelung River, respectively.

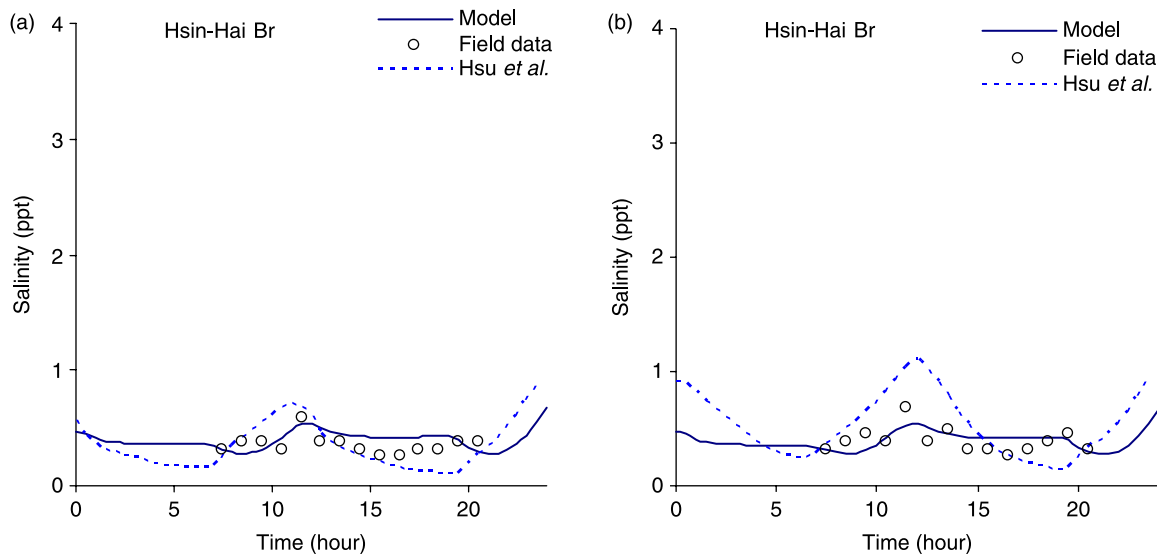


**Figure 7** | Comparison of measured and simulated salinities on 24 June 1994 at (a) Hsin-Hai bridge (1 m below surface water); and (b) Hsin-Hai bridge (2.5 m below surface water).

**Table 3** | AME of simulated time series of salinity for different stations/layers on 24 June 1994

	Hsin-Hai	Taipei	Pa-Ling
Surface	0.09	0.43	0.45
Bottom	0.08	0.52	0.4

For the  $Q_{90}$  condition, in contrast to the  $Q_{mean}$  condition, the results for spring and neap tides are almost the same. This is due to the presence of the topographic sills at the upriver end of the tributaries, which prevents the salinity intrusion during low freshwater discharge conditions. The simulations for averaged spring-neap tide indicate that discharge reduction from  $Q_{mean}$  to  $Q_{90}$  results in increasing salinity intrusions about 8 km, 7.5 km and 6.5 km in the bottom layer of Tahan Stream, Hsintien Stream and Keelung River, respectively.

Liu et al. (2007) used a 3D model with a mixing length closure scheme to obtain an exponential correlation between tidally averaged salt intrusion length and freshwater discharge in this system. Here, simulations were carried out to achieve a power correlation between the maximum salinity intrusion length and fresh water discharge for the spring tide (Figure 8). The following equations were obtained for the maximum salinity intrusion length  $L$  as a function of  $Q$  at each tributary:

$$L = 38.0 \times Q^{-0.22}; \quad R^2 = 0.93 \tag{4}$$

$$L = 23.6 \times Q^{-0.17}; \quad R^2 = 0.94 \tag{5}$$

$$L = 41.5 \times Q^{-0.14}; \quad R^2 = 0.99 \tag{6}$$

for Tahan Stream, Keelung River and Hsintien Stream, respectively.

These findings are supported by previous theoretical, numerical and field studies (e.g. Hetland & Geyer 2004). Theoretical arguments of Monsmith et al. (2002, Equations (12–14)) have shown that the power of  $Q$  should be  $-0.33$

**Table 4** | Freshwater discharges ( $m^3/s$ ) used for scenarios

	$Q_{mean}$	$(Q_{mean} + Q_{75})/2$	$Q_{75}$	$(Q_{75} + Q_{90})/2$	$Q_{90}$
Tahan Stream	62.1	32.13	8.15	6.08	4
Hsintien Stream	72.7	46.45	20.2	13.55	6.9
Keelung River	26.1	14.86	3.61	2.46	1.3

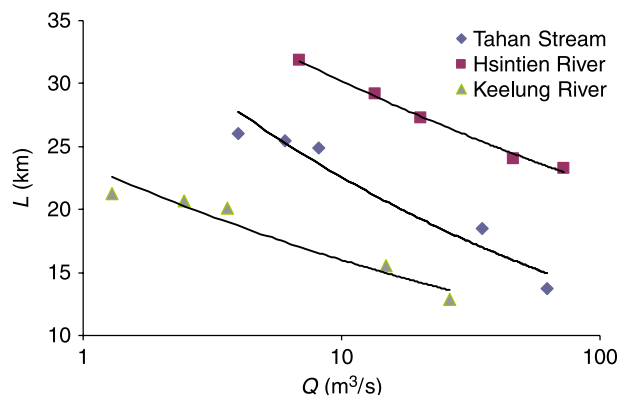


**Figure 8** | Correlation between maximum salinity intrusion length and upstream river discharge.

while Oey (1984) stated that in the Hudson River the length of salinity intrusion is correlated to  $Q^{-0.20}$ . The field measurements in the San Francisco bay also showed  $L \sim Q^{-0.15}$ , a departure from the theory (Monsmith et al. 2002). They argued that the observed weaker dependence on river discharge is due to the variable bathymetry and the effects of stratification on vertical mixing. In addition, recent numerical experiments in the Arvand River (Zahed et al. 2008) also showed that  $L \sim Q^{-0.20}$ . The relatively weaker dependence of salinity intrusion length to the river discharge in the tributaries could be due to the complexity of the system. Here, the salinity intrusion in each tributary depends on the discharges of all three tributaries.

The high correlation factors derived indicate that fresh water discharge plays an important role in salinity intrusion in Danshuei River estuary. These equations can be used as rapid tools for prediction of the effect of any fresh water discharge variations on salinity intrusion length.

## CONCLUSIONS

A 2D numerical model was calibrated, verified and then used to investigate the salinity intrusion variation under different fresh water discharges. Measured water levels were used for calibration of the model while the measured velocities at different levels were used for verification of the hydrodynamic processes. The measured salinities at different stations were then used for calibration and verification of mixing processes.

The following conclusions were made.

1. The sigma coordinate model using a  $k - \epsilon$  closure scheme simulates both the hydrodynamic and mixing processes in the Danshuei estuarine system well.
2. During  $Q_{\text{mean}}$  conditions, salt water rarely intrudes in Hsintien Stream. On the other hand, salinity intrusion during spring tides is about 2–3 km greater than those during neap tides.
3. The magnitude of freshwater discharge is the main parameter affecting the salinity intrusion in Danshuei River estuary. Using different hydrological conditions, simple equations were suggested for the maximum salinity intrusion  $L$  due to fresh water discharge (Equations (4–6)). These equations can be used to predict the effect of fresh water discharge on salinity intrusion length.

## ACKNOWLEDGEMENTS

We are grateful to Taiwan Water Resources Agency for providing the field data. Thanks are also extended to Dr K. Olesen from DHI and to A. Shahkolahi, J. Parsa and H. Moshfeghi for helpful discussions. Finally, we thank the anonymous reviewers whose valuable comments helped us to improve the manuscript.

## REFERENCES

- Abbott, M. B. & Ionescu, F. 1967 On the numerical computation of nearly-horizontal flows. *J. Hydr. Res.* **5**(2), 97–117.
- Attrill, M. J. 2002 A testable linear model for diversity trends in estuaries. *J. Anim. Ecol.* **71**(2), 262–269.
- Dyer, K. R. 1997 *Estuaries: A Physical Introduction*. John Wiley and Sons, New York.
- Fischer, H., List, J., Koh, R., Imberger, J. & Brooks, N. 1979 *Mixing in inland and coastal waters*. Academic Press, New York, pp. 483.
- Hetland, R. & Geyer, W. 2004 An idealized study of the structure of long, partially mixed estuaries. *J. Phys. Oceanogr.* **34**, 2677–2691.
- Hsu, M. H., Kuo, Y., Kuo, J. T. & Liu, W. C. 1999 Procedure to calibrate and verify numerical models of estuarine hydrodynamics. *J. Hydr. Eng.* **125**(2), 166–182.
- Jakobsen, F., Olesen, K. W. & Madsen, M. 2005 A simple method to include vertical resolution in a river model, and results from an implementation. *Nord. Hydrol.* **36**, 163–174.
- Jassby, A., Kimmerer, W., Monismith, S., Armor, C., Cloern, J., Powell, T., Schubel, J. & Vendliniski, T. 1995 Isohaline position as a habitat indicator for estuarine populations. *Ecol. Appl.* **5**, 272–289.
- Liu, W. C., Hsu, M. H. & Kuo, A. Y. 2001 Investigation of long-term transport in Tanshui River Estuary, Taiwan. *J. Water Port Coast. Ocean Eng.* **127**(2), 61–70.
- Liu, W. C., Chen, W. B., Cheng, R. H., Hsu, M. H. & Kuo, A. Y. 2007 Modeling the influence of river discharge on salt intrusion and residual circulation in Danshuei River Estuary, Taiwan. *Cont. Shelf Res.* **27**, 900–921.
- Monismith, S., Kimmerer, W., Burau, J. & Stacey, M. 2002 Structure and flow-induced variability of the subtidal salinity field in Northern San Francisco Bay. *J. Phys. Oceanogr.* **32**, 3003–3019.
- Oey, L. Y. 1984 On steady salinity distribution and circulation in partially mixed and well mixed estuaries. *J. Phys. Oceanogr.* **14**, 629–645.
- Remane, A. & Schlieper, C. 1971 *Biology of Brackish Water*, Schweizerbartsche Verlagsbuchhandlung, Stuttgart.
- Rodi, W. 1987 Examples of calculation methods for flow and mixing in stratified fluids. *J. Geophys. Res.* **92**(C5), 5305–5328.
- Slørdal, L. H. 1997 The pressure gradient force in sigma-coordinate ocean models. *Int. J. Numeric. Meth. Fluids* **24**, 987–1017.
- US Army Corps of Engineers 1991 *Tidal Hydraulics, Engineer Manual*, EM 1110-2-1607, Washington, DC, pp. 2.1–3.5.
- Van Der Tuin, H., Mikhailov, V., Roelfzema, A. & Volker, A. 1991 *Guidelines on the Study of Sea Water Intrusion into Rivers*. UNESCO, France.
- Zahed, F., Etemad-Shahidi, A. & Jabbari, F. 2008 Modeling of salinity intrusion under different hydrological condition in Arvand River Estuary. *Can. J. Civil Eng.* (In press).

First received 19 June 2007; accepted in revised form 19 June 2008